RSC Advances

ROYAL SOCIETY OF CHEMISTRY

www.rsc.org/advances

Journal Name

RSCPublishing

ARTICLE

Cellulose-based Hydrophobic Carbon Aerogels as Versatile and Superior Adsorbents for Sewage Treatment

Cite this: DOI: 10.1039/x0xx00000x

Haiyan Wang, Yutong Gong and Yong Wang*[a]

Received 00th January 2012,
Accepted 00th January 2012

DOI: 10.1039/x0xx00000x

www.rsc.org/

Carbon aerogels have attracted considerable attention in fundamental investigation and potential applications in a myriad of fields. We present a novel approach for the synthesis of cellulose-based carbon aerogels by dissolution, gelation, regeneration, freeze-drying and carbonization of cellulose. The carbon aerogels obtained here possess the characteristics of high surface area (500 $m^2 g^{-1}$), hydrophobicity, and fire-resistance. In addition, the carbon aerogels show excellent adsorption capacity and selectivity for removal of oils, organic solvents, a variety of dyes, and heavy ions, so they could be used as promising adsorbents for sewage treatment. Especially for malachite green and Cu (II), the adsorption capacities can reach up to 1947 mg g^{-1} and 801 mg g^{-1}, respectively, which far surpass other aerogels previous reported.

Introduction

Carbon aerogels, which possess abundant interconnected micropores or macropores, are lightweight, highly porous amorphous nanomaterials.[1, 2] They feature a multitude of unique properties such as low density, high porosity, large specific surface area, and excellent electrical conductivity.[3-8] As a result, three-dimensional carbon aerogels demonstrate wide applications in various fields, covering from hydrogen storage materials,[9-11] catalyst supports,[12-16] gas sensors,[17-19] supercapacitors,[20-24] to sewage treatment.[25-27] In particular, ultralight carbon nanofiber aerogels have shown high flexibility that was superior to conventional low-density, high-porosity materials. Such materials with unique structures can be immediately adopted as super adsorbents, as illustrated by Antonietti [28], Sun[29] and Yu.[30]

Organic aerogels are representatives of the precursors of carbon aerogels.[31-34] Traditionally, they were prepared from polymer monomer through sol-gel, followed by acetone exchange and supercritical CO_2 drying. Several kinds of organic aerogels have been reported. For example, resorcinol-formaldehyde aerogels,[35, 36] phenol-melamine-formaldehyde aerogels,[37] phenol-formaldehyde aerogels.[38] Then these organic aerogels were carbonized in an inert atmosphere to obtain three-dimensional porous carbon aerogels. However, commercialization of these carbon aerogels is limited for the toxic precursors, tedious preparation processes, and long preparation period. Recently, some attempts such as CNT aerogels,[18, 20, 39] graphene aerogels,[3, 22] CNT/graphene aerogels,[40] carbon nanofiber aerogels,[30, 41] magnetic Fe_2O_3/carbon foam,[42] and other carbon-based nanostructured materials have been prepared to overcome these shortcomings. They often exhibit prominent properties such as ultra-flyweight property, high porosity of >98%, high electrical conductivity or high adsorption capacities. However, expensive equipment and high fabrication costs and complex processes are the primary obstacles for further industrialization of these carbon aerogels.

In the 21st century, biomass materials, derived from plants and organisms, have been promising raw materials for preparing carbon materials due to their low costs, sustainability, biocompatibility, and biodegradability. For example, sulfur or nitrogen doped carbon aerogels with enhanced electrocatalytic activity in oxygen reduction reaction have been obtained by hydrothermal carbonization of glucose in the presence of a kind of protein, ovalbumin, as reported by Antonietti et al.[43] But hydrothermal carbonization in autoclave needs high temperature and high pressure which restrict its applications. Especially, the processes can't be observed intuitively, so the mechanisms are difficult to explain. Though glucose as natural biomass material is wide spread and renewable, as its upper raw material, cellulose is of more research significance. Recently, carbon nanofiber aerogel was made through pyrolyzing raw cotton.[29] Though the obtained carbon nanofiber aerogel shows excellent adsorption capacity, the use of cotton as a carbon resource limited its application.

Cellulose is the oldest and the most abundant natural raw material in the world, which has shown excellent performances in a wide range of applications. Therefore, finding a usual method to obtain carbon aerogel from cellulose is of some significance. Cellulose aerogels, as the 'young' generation succeeding the silica and polymer aerogels, are intriguing materials with high percentage of large mesopores and small macropores, low density, and biocompatibility. Several attempts to prepare cellulose aerogels have been reported.[44-48] Highly porous cellulose aerogels can be prepared by dissolution /regeneration of cellulose in different solution system, followed by solvent exchange and freezing-drying or supercritical CO_2 drying.[49] Due to the strong intra and inter molecular hydrogen bonds interactions, cellulose possesses high orientation and crystallinity, hardly dissolves in ordinary solvents. However,

including $Ca(SCN)_2$,[45] N,N-dimethylacetamide (DMAc)/LiCl,[47] dimethylsulfoxide (DMSO)/LiCl,[44] especially N-methylmorpholine-N-oxide (NMMO)[46] are demonstrated to be good solvents of cellulose. For example, Zhang et al. reported LiOH/urea and NaOH/urea aqueous solutions precooled to -12 ^{o}C could be used to obtain cellulose solution within 2 min.[49] Compared with NaOH/urea system, the hydrogels obtained from LiOH/urea system were of higher strength and more transparent because the type of alkali may affect the regeneration behavior.

Herein, a novel way to fabricate cellulose-based carbon aerogels was developed by using LiOH/urea system, sol-gel, lyophilization, and carbonization at 800 ^{o}C in N_2. The as-prepared cellulose aerogels exhibit low BET surface area. However, after carbonization under high temperature, the BET surface area of the as made aerogel increased remarkably and they show low density (20 mg cm^{-3}), high porosity (98%). Moreover, the morphology, structure and properties were studied by various techniques. Surprisingly, when used as absorbents, cellulose-based carbon aerogels with hydrophobic properties show outstanding absorption capacity, recyclability and selectivity. Cellulose-based aerogels can absorb a variety of oils and organic solvents. Besides, they can remove organic dyes and heavy ions from water. The absorption capacity of malachite green and Cu (II) can reach up to 1947 mg g^{-1} and 801 mg g^{-1}. So we believe cellulose-based carbon aerogels can be prominent candidates for efficient absorbents in water purification or other environmental applications.

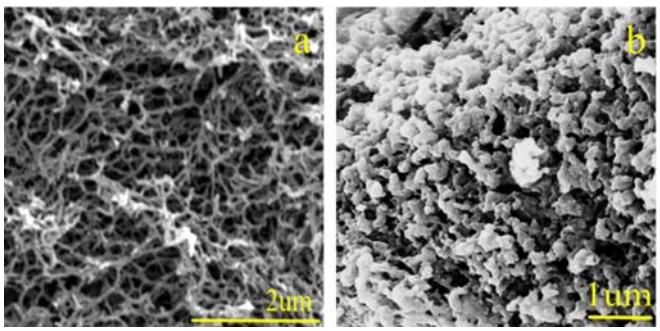

Figure 1. SEM images of cellulose aerogel (a), carbon aerogel (b).

Experimental

Materials.

α-Cellulose (particle size : 25 um), lithium hydroxide monohydrate (98%), and urea (99%) were purchased from Aladdin Industrial Corporation. Other organic agents and the heavy metal salts used were all purchased from Aladdin or Sinopharm Chemical Reagent Co., Ltd. The dyes, methyl blue (MB), alizarin yellow (AY), methyl orange (MO), methylene blue (MEB), calcein (CA), amido black 10B (AB), malachite green (MG), rose Bengal (RB) were also purchased from Aladdin Industrial Corporation.

Characterization.

The microstructures of cellulose aerogels and carbon aerogels were characterized by scanning electron microscope (SEM) images and transmission electron microscope (TEM). SEM analysis was performed on a Hitachi S-4800 electron microscope at an accelerating voltage of 25.0 kV. TEM analysis was obtained via a JEM-1230 instrument at an accelerating voltage of 80 kV. The diffraction (XRD) data were collected with a D/tex-Ultima TV wide angle X-ray diffractometer equipped with Cu Kα radiation (λ=1.54 Å). The X-ray photoelectron spectra (XPS) were carried out on an ESCALAB MARK II spherical analyzer using aluminum-magnesium binode (Al 1486.6 eV, Mg 1253.6 eV) X-ray source. FT-IR spectra were recorded on a Nicolet Fourier transform infrared spectroscopy. The elemental analysis was tested on th Flash EA 1112, ThermoFinnigan. The BET specific surface area was calculated by a multipoint method based on the adsorption data and the pore size was obtained using the Barret-Joyner-Halender (BJH) method based on the adsorption data.

Synthesis of cellulose aerogels.

Cellulose aerogels were prepared according to previously reported procedure by Zhang group.[49] We choose aqueous LiOH/urea/H_2O (4.6:19:76.4 w/w) rather than aqueous LiOH/urea/H_2O (4.6:15:80.4 w/w) due to the different cellulose sample we used. 3 wt% cellulose was dispersed in the solvent mixture LiOH/urea/H_2O (4.6:19:76.4 w/w) precooled to -12 ^{o}C and stirred for 10 min at ambient temperature to obtain a transparent cellulose solution. The cellulose solution was subjected to centrifugation. Then the resulting solution was immersed in t-BuOH for regeneration at 20 ^{o}C for 2 h. The cellulose hydrogel was exchanged with deionized water, EtOH, t-BuOH using dialysis bag. Each repeated for several times, followed by nitrogen freeze-drying.

Preparation of carbon aerogels.

The cellulose aerogels were finally carbonized at 400 ^{o}C for 1h then 800 ^{o}C for 1 h (heating rate of 5 ^{o}C/min) under nitrogen to obtain carbon aerogels.

Solvent and oil absorption of carbon aerogels.

The absorption capacity (Q) of carbon aerogels towards different solvents and oils with different densities were tested, including furfural, methyl benzene, chloroform, dimethyl formamide (DMF), pump oil, cyclohexane, sobean oil, acetone, petroleum ether, and phenoxin. The samples were immersed into different oils, and took out for measurements. The carbon aerogels before and after absorption were weighed as W_i and W_e. Thus Q value was calculated as follows: $Q = (W_e - W_i)/W_i$. The regeneration of absorption capacity was investigated in the same way after the oil-saturated carbon aerogels were dried in an oven at 70 ^{o}C.

Dye adsorption of carbon aerogels.

Carbon aerogels were put into a variety of dye aqueous solutions such as MB, AY, MO, MEB, CA, AB, MG and RB. The dye aqueous solutions were stirred at room temperature until the absorption equilibrium was achieved. The concentration of the solution was tested by UV-vis spectra. The equilibrium adsorption capacity (Q_{eq}) was calculated through the following equation: $Q_{eq} = (C_i - C_{eq})\ V\ M_d / W_{CA}$, where, C_i and C_{eq} are the initial and final concentration of the dye aqueous solution. V is the volume of the dye solution and M_d is the molecular weight of the dye. W_{CA} is the weight of the carbon aerogel added into the dye solution.

Heavy ion adsorption of carbon aerogels.

10 mg carbon aerogels were added to 25 ml heavy ion solutions with concentration of 400 mg/L. The solutions were stirred at room temperature for 12 h to achieve the adsorption equilibrium. The remaining concentrations of heavy ions were measured by ICP-AES technique.

Results and Discussion

Morphology of the carbon aerogel.

SEM micrographs of the cellulose aerogel showed a homogeneous, porous, interconnected 3D network structure, which was formed during the self-assembly process of cellulose molecules (Figure 1a). The cellulose aerogel was composed of interconnected fibrils whose diameter was about 20 nm wide. After carbonization, it was obvious that the porous 3D network was maintained (Figure 1b). But compared with the cellulose aerogel, the structure of the carbon aerogel contracted upon itself and the pore structure packed, giving rise to smaller pore diameter. Such phenomenon can be demonstrated by the representative TEM micrographs of the cellulose aerogel and its carbonized counterpart (see the supporting information, Figure S 1a, S 1b).

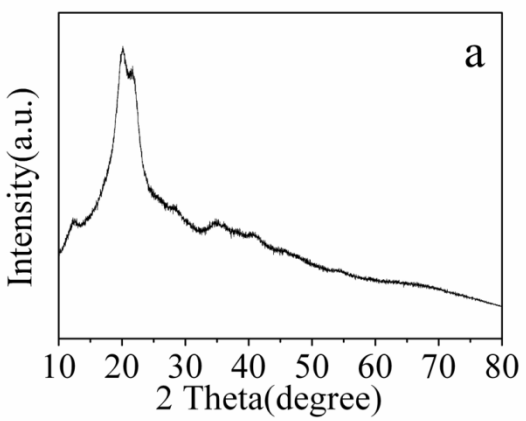

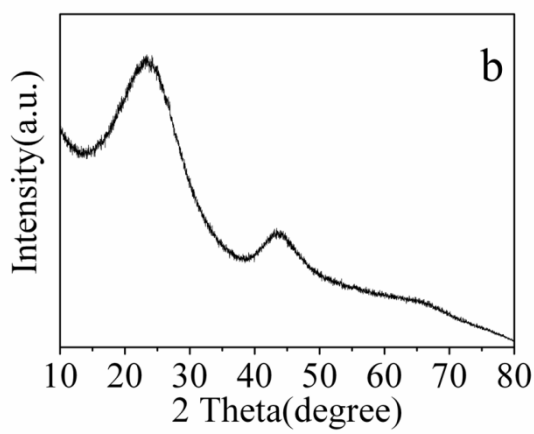

Figure 2. X-Ray diffraction profiles of cellulose aerogel (a), carbon aerogel (b).

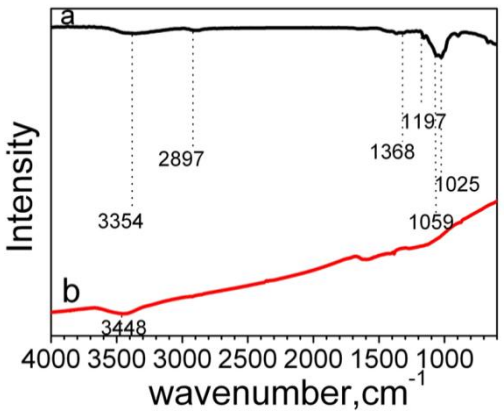

Figure 3. FT-IR spectra of cellulose aerogel (a), and carbon aerogel (b).

The pore structures of the cellulose aerogel and carbon aerogel were both investigated with nitrogen sorption measurements (see the supporting information, Figure S2a). The S_{BET} value of the cellulose aerogel (149 $m^2 g^{-1}$) was mainly contributed by large mesopores (30-50 nm) and the t-Plot micropore area was only 3 $m^2 g^{-1}$. Nevertheless, The S_{BET} value of the carbon aerogel (500 $m^2 g^{-1}$) was owing to the increase of micropores at the expense of the macropores. BJH method was used to determine the pore size distribution and the volumes of meso and micropores. According to the information showed in Figure S2b of the Supporting Information, the mean pore diameter after carbonization decreased from the initial 15 nm to 5 nm, which corresponded to the SEM and TEM images, and the volume of micropores after carbonization increased greatly to 0.19 $cm^3 g^{-1}$.(see the supporting information, Figure S3)

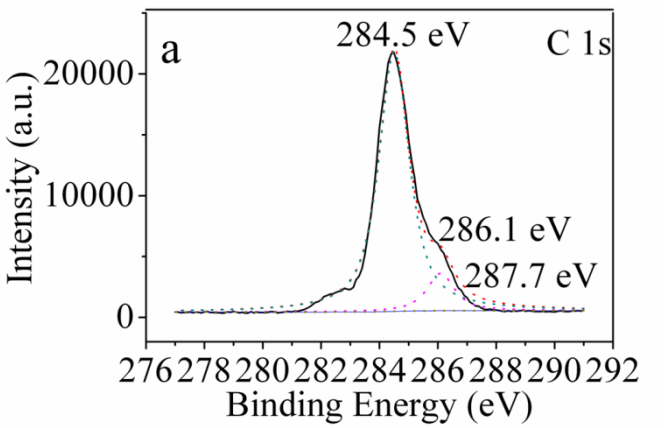

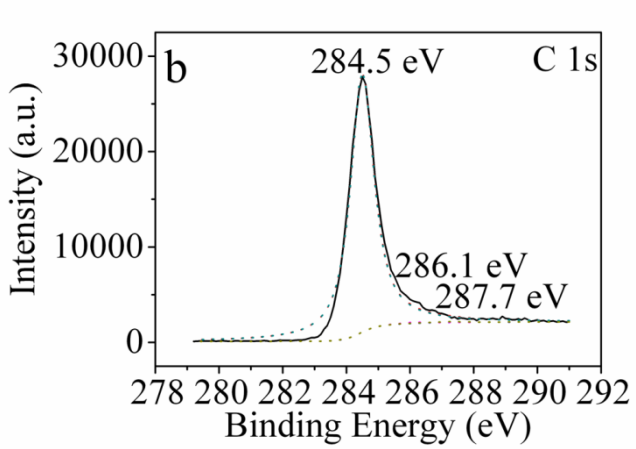

Figure 4. XPS C1s spectra of cellulose aerogel (a) and carbon aerogel (b).

XRD and FT-IR of the cellulose aerogel and carbon aerogel.

To understand the nature of the cellulose aerogel and the effect of carbonization, we investigated the X-ray diffraction (XRD) patterns of the cellulose aerogel and its carbon aerogel (Figure 2a, 2b). The original cellulose aerogel showed three peaks centered at 12.4°, 20.1°, 21.7°, corresponding to the typical $(1\bar{1}0)$, (110), (200) planes which indicated a typical cellulose II crystalline was formed.[50] After carbonization, these peaks disappeared, thus indicating the crystalline of the cellulose aerogel was destroyed and peaks at 23.4°, 43.5° corresponding to the (002), (100) planes of graphite were broadened, meaning amorphous carbon was formed. The effect of carbonization was also examined by Fourier transformation infrared (FTIR) spectra (Figure 3). The broad and strong band at 3354 cm^{-1} and 2897 cm^{-1} are attributed to the O-H and C-H stretching vibrations of cellulose aerogels, respectively. The band at 1368 cm^{-1} can be ascribed to C-H deformation vibration. The C-O-C stretching vibration bands appear at 1197 cm^{-1}, 1059 cm^{-1}, 1025 cm^{-1}. After carbonization, the strong peaks of functional groups, such as O-H, C-H, C-O, became weaker. Some even disappeared. The X-ray photoelectron diffraction (XPS) was also applied to explain the elements' states. As can be seen in Figure 4, the C 1s peak can be decomposed into three spectral peaks: C-C at 284.5 eV, C-OH at 286.1 eV, and C=O at 287.5 eV. Compared Figure 4a and Figure 4b, the intensity peaks characteristic of the C-OH groups decreased, indicating that after carbonization, the content of oxygen decreased. These results can be identified by elemental analysis experiment. As shown in Table 1, the O element content and H element content in the carbon aerogel are decreased apparently after the carbonization of cellulose aerogels.

Table 1. Elemental content of cellulose aerogel and carbon aerogel

Elemental composition	Cellulose aerogel	Carbon aerogel
wt% C	42.4	91.8
wt% O	51.2	7.7
wt% H	6.4	0.5

Absorption properties of carbon aerogel.

Due to their low density (20 mg cm^{-3}), high porosity (98%), high surface area (500 m^2 g^{-1}), and hydrophobicity, the carbon aerogels have shown distinguished performance on absorbing oils and organic solvents without suction of water, which could be ideal candidates for waste water purification and marine oil-spill recovery. The photographs in Figure 5a show the fast process of the aerogel absorbing a layer of toluene labeled with Sudan III dye on the water surface under the capillary effect. It was proved when the carbon aerogel contacted with toluene, the organic solvent was absorbed within one second (demonstration Movie 1 provided in the supporting information). To investigate the absorption capacity of the carbon aerogels, it was tested in various kinds of oils and organic solvents, such as hydrocarbons (cyclohexane, acetone, etc.), halides (chloroform, phenixin), aromatic compounds (toluene), and commercial oils (pump oil, soybean oil), which all are common pollutants in our daily life or industry manufacture wastes. As shown in Figure 5b, the maximum adsorption capacity of phenixin was 25 times of its weight, which was higher than for other porous materials, such as Fe/C (ca. 10 times), PU sponge (ca. 20 times).[51] Recyclability of the carbon aerogels has a significant influence in sewage purification application. Figure 5c shows the recycle use of the carbon aerogels for adsorption of phenixin. After five cycles, no obvious change of the saturated adsorption capacity was found, indicating good recyclability, which may be owing to the stable 3D porous structure of the carbon aerogels. Meanwhile, it exhibited prominent fire-resistance when the oil-saturated carbon aerogel exposed to an alcohol flame (Figure 5d, 5e). Both the morphology and micro-porous structure remained the same with the original carbon aerogel (see supporting information, Figure S4, S5). So we believe the oils and organic solvents absorbed can be removed through evaporation or burning in oil/chemical cleanup applications.

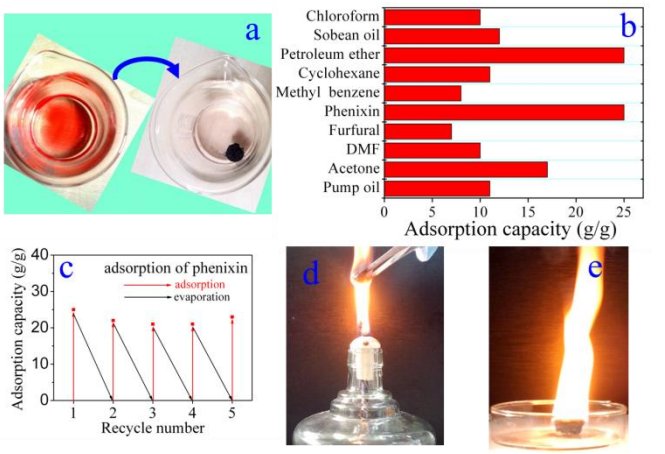

Figure 5. a) Adsorption process of toluene (labeled with Sudan III dye) on water by carbon aerogels within one second. b) Adsorption capacities of the carbon aerogels for a range of organic solvents and oils. c) Regeneration capacity of the carbon aerogels for adsorbing phenixin. Phenixin can be removed by putting the aerogel in the oven at 70 °C for recycled use. d and e) Photographs of burning the oil saturated carbon aerogels.

In addition, it was found that the carbon aerogels were effective for both basic and acid dyes adsorption. When carbon aerogels were added to the dye solutions, the solutions eventually turned clear (Figure 6a). The tests showed that the carbon aerogels exhibited high adsorption rate when the Rose Bengal solution got through them, the dripping solution were clear (demonstration Movie 2 provided in the supporting

information). The adsorption capacities of different dyes range from 195 to 1947 mg g^{-1}, which greatly exceeded traditional adsorbents and other reported porous aerogels, such as graphene aerogels, CNT aerogels, graphene/CNT hybrid aerogels, CNFs (Figure 6b).[41, 52, 53] The carbon aerogels demonstrate much better adsorption capacity for basic dyes, such as MG, MEB. Its adsorption capacity for Methylene blue was 1192 mg g^{-1}, superior to the other carbon adsorbents including the commercial activated carbon (Figure 6c).[41, 52, 54] The super dye adsorption capacity may have much to do with the unique pore structure and its hydrophobic property. The unique pore structure such as the large amount of the micropores, and the mean pore sizes (5 nm) may be in favor of the adsorption of the micromolecules. Besides, because of the hydrophobicity, water can be prevented from filling the pores, leading to making full use of the pores. The adsorption capacity for malachite green was extremely prominent, compared with the other adsorbents reported including AC from pine sawdust (370 mg g^{-1}), carbonaceous material (75 mg g^{-1}), graphene aerogels (550 mg g^{-1}) and so on.[52, 55] To our surprise, the carbon aerogels could even adsorb Methyl blue, which was hardly proved by other reports. However, the above adsorption results in the literature were recorded under optional condition. So we believe the adsorption capacity results can be improved by selecting the optimal PH value and the initial dye concentration. In this respect, the hydrophobic and porous carbon aerogels can be used as high-efficient adsorbents for dye removal from sewage. Furthermore, given the serious water pollution caused by heavy ions, many efficient adsorbents, including thiol-functionalized Zn-doped biomagnetite particles,[56] magnetite-reduced graphene oxide composites,[57] nanoparticle film of copper hexacyanoferrate,[58] and so on. The excellent adsorption capacity and selectivity of the carbon aerogels were further confirmed by heavy metals removal. The adsorption behaviors of the carbon aerogels for a variety of heavy ions were reflected in Figure 6d. The calculated maximum adsorption capacities for Cu (II) and Sn (II) were 801 mg g^{-1} and 183 mg g^{-1}, respectively, which far surpass that of graphene aerogel, graphene/MWCNT aerogel, magnetic chitosan beads and hybrid mesoporous materials for Cu (II).[53, 59, 60] However, the carbon aerogels didn't show adsorption performance for Zn (II) and Ni (II) at all. Thus based on the preeminent adsorption capacity and selectivity for removal of heavy ions, the carbon aerogels are promising adsorbents in water purification.

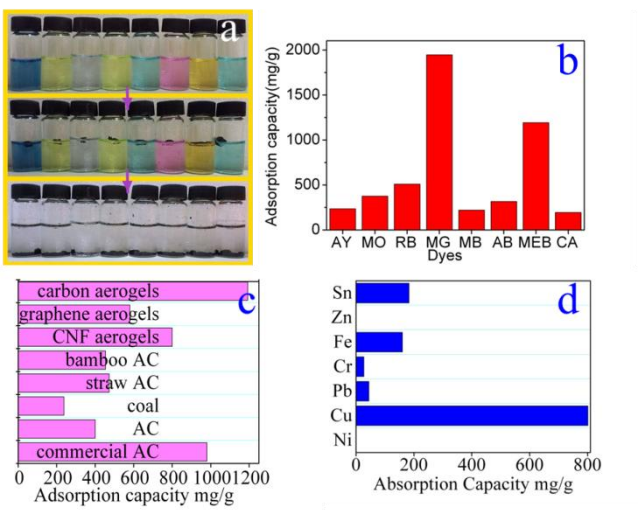

Figure 6. a) Photograph of dyes before and after adsorption by carbon aerogels. b) Adsorption capacities of carbon aerogels for a range of dyes. c) A comparison of adsorption capacity for methylene blue with other carbon adsorbents. d) Adsorption capacities of carbon aerogels for a variety of heavy ions.

Conclusions

In conclusion, a novel method for the transforming of cellulose into fire-resistant, and highly porous carbon aerogels was developed in this paper, which involved LiOH/urea system, sol-gel, freeze-drying, and carbonization. The method is characterized by available rich raw material sources, low cost and environmentally friendly procedure. The carbon aerogels show great potential for sewage purification when used as oils and organic solvents adsorbents, the high efficient removal agents of different dyes and heavy metals. We believe the carbon aerogels are promising for treating sewage in most industrial fields.

Acknowledgements

Financial support from the National Natural Science Foundation of China (21376208 & U1162124), the Zhejiang Provincial Natural Science Foundation for Distinguished Young Scholars of China (LR13B030001), the Specialized Research Fund for the Doctoral Program of Higher Education (J20130060), the Fundamental Research Funds for the Central Universities, the Program for Zhejiang Leading Team of S&T Innovation, the Partner Group Program of the Zhejiang University, and the Max-Planck Society are greatly appreciated.

Notes and references

[a] Carbon Nano Materials Group, Center for Chemistry of High-Performance and Novel Materials, Department of Chemistry Zhejiang University, Hangzhou 310028, P. R. China. Fax: 86-571-8795-1895; Tel: 86-571-8827-3551; E-mail: chemwy@zju.edu.cn.

Electronic Supplementary Information (ESI) available: [TEM images and N_2 adsorption/desorption isotherms and pore size distributions of the cellulose aerogel and carbon aerogel, the morphology and micro-porous structures of the carbon aerogel before and after burning, adsorption of movies, Figure S1 – S5, Movie 1 and Movie 2]. See DOI: 10.1039/b000000x/

1. M. Antonietti, N. Fechler and T.-P. Fellinger, *Chem. Mater.*, 2013, **26**, 196-210.
2. J. Lee, J. Kim and T. Hyeon, *Adv. Mater.*, 2006, **18**, 2073-2094.
3. Y. Zhao, C. Hu, Y. Hu, H. Cheng, G. Shi and L. Qu, *Angew. Chem. Int. Ed.*, 2012, **51**, 11371-11375.
4. J. M. Romo-Herrera, M. Terrones, H. Terrones, S. Dag and V. Meunier, *Nano Letters*, 2006, **7**, 570-576.
5. D. Wu, R. Fu, S. Zhang, M. S. Dresselhaus and G. Dresselhaus, *Carbon*, 2004, **42**, 2033-2039.
6. A.-H. Lu, G.-P. Hao and Q. Sun, *Angew. Chem. Int. Ed.*, 2013, **52**, 7930-7932.
7. N. Husing and U. Schubert, *Angew. Chem. Int. Ed.*, 1998, **37**, 23-45.
8. M. A. Worsley, P. J. Pauzauskie, T. Y. Olson, J. Biener, J. H. Satcher and T. F. Baumann, *J. Am. Chem. Soc.*, 2010, **132**, 14067-14069.
9. H. Kabbour, T. F. Baumann, J. H. Satcher, A. Saulnier and C. C. Ahn, *Chem. Mater.*, 2006, **18**, 6085-6087.

10.J. Biener, M. Stadermann, M. Suss, M. A. Worsley, M. M. Biener, K. A. Rose and T. F. Baumann, *Energy Environ. Sci.*, 2011, **4**, 656-667.
11.H. Y. Tian, C. E. Buckley, S. B. Wang and M. F. Zhou, *Carbon*, 2009, **47**, 2128-2130.
12.P. Zhang, J. Yuan, T.-P. Fellinger, M. Antonietti, H. Li and Y. Wang, *Angew. Chem. Int. Ed*, 2013, **52**, 6028-6032.
13.P. Zhang, Y. Gong, H. Li, Z. Chen and Y. Wang, *Nature Commun.*, 2013, **4**, 1593.
14.C. Moreno-Castilla and F. J. Maldonado-Hódar, *Carbon*, 2005, **43**, 455-465.
15.C. Zhao, Y. Kou, A. A. Lemonidou, X. Li and J. A. Lercher, *Angew. Chem. Int. Ed.*, 2009, **48**, 3987-3990.
16.W. Deng, M. Liu, X. Tan, Q. Zhang and Y. Wang, *J. Catal.*, 2010, **271**, 22-32.
17.S. Peng and K. Cho, *Nano Letters*, 2003, **3**, 513-517.
18.Z. Zanolli, R. Leghrib, A. Felten, J.-J. Pireaux, E. Llobet and J.-C. Charlier, *ACS Nano*, 2011, **5**, 4592-4599.
19.J. Zou, J. Liu, A. S. Karakoti, A. Kumar, D. Joung, Q. Li, S. I. Khondaker, S. Seal and L. Zhai, *ACS Nano*, 2010, **4**, 7293-7302.
20.M. F. L. De Volder, S. H. Tawfick, R. H. Baughman and A. J. Hart, *Science*, 2013, **339**, 535-539.
21.H.-C. Chien, W.-Y. Cheng, Y.-H. Wang and S.-Y. Lu, *Adv. Fun. Mater.*, 2012, **22**, 5038-5043.
22.Z.-S. Wu, A. Winter, L. Chen, Y. Sun, A. Turchanin, X. Feng and K. Müllen, *Adv. Mater.*, 2012, **24**, 5130-5135.
23.Z.-S. Wu, Y. Sun, Y.-Z. Tan, S. Yang, X. Feng and K. Müllen, *J. Am. Chem. Soc.*, 2012, **134**, 19532-19535.
24.X.-L. Wu, T. Wen, H.-L. Guo, S. Yang, X. Wang and A.-W. Xu, *ACS Nano*, 2013, **7**, 3589-3597.
25.G. S. Simate, S. E. Iyuke, S. Ndlovu, M. Heydenrych and L. F. Walubita, *Environ. Int.l*, 2012, **39**, 38-49.
26.S. Kar, R. C. Bindal and P. K. Tewari, *Nano Today*, 2012, **7**, 385-389.
27.D. D. Nguyen, N.-H. Tai, S.-B. Lee and W.-S. Kuo, *Energy Environ. Sci.*, 2012, **5**, 7908-7912.
28.T.-P. Fellinger, R. J. White, M.-M. Titirici and M. Antonietti, *Adv. Fun. Mater.*, 2012, **22**, 3254-3260.
29.H. Bi, Z. Yin, X. Cao, X. Xie, C. Tan, X. Huang, B. Chen, F. Chen, Q. Yang, X. Bu, X. Lu, L. Sun and H. Zhang, *Adv.Mater.*, 2013, **25**, 5916-5921.
30.Z.-Y. Wu, C. Li, H.-W. Liang, J.-F. Chen and S.-H. Yu, *Angew. Chem. Int. Ed.*, 2013, **52**, 2925-2929.
31.S. Mulik, C. Sotiriou-Leventis and N. Leventis, *Chem. Mater.*, 2008, **20**, 6985-6997.
32.W. Li, G. Reichenauer and J. Fricke, *Carbon*, 2002, **40**, 2955-2959.
33.J. Yamashita, T. Ojima, M. Shioya, H. Hatori and Y. Yamada, *Carbon*, 2003, **41**, 285-294.
34.M. Mirzaeian and P. Hall, *J. Mater. Sci.* 2009, **44**, 2705-2713.
35.S. A. Al-Muhtaseb and J. A. Ritter, *Adv. Mater.*, 2003, **15**, 101-114.
36.A. M. ElKhatat and S. A. Al-Muhtaseb, *Adv. Mater.*, 2011, **23**, 2887-2903.
37.D. Long, J. Zhang, J. Yang, Z. Hu, G. Cheng, X. Liu, R. Zhang, L. Zhan, W. Qiao and L. Ling, *Carbon*, 2008, **46**, 1259-1262.
38.A. Szczurek, K. Jurewicz, G. Amaral-Labat, V. Fierro, A. Pizzi and A. Celzard, *Carbon*, 2010, **48**, 3874-3883.
39.X. Gui, J. Wei, K. Wang, A. Cao, H. Zhu, Y. Jia, Q. Shu and D. Wu, *Adv. Mater.*, 2010, **22**, 617-621.
40.H. Sun, Z. Xu and C. Gao, *Adv. Mater.*, 2013, **25**, 2554-2560.
41.H.-W. Liang, Q.-F. Guan, L.-F. Chen, Z. Zhu, W.-J. Zhang and S.-H. Yu, *Angew. Chem. Int. Ed.*, 2012, **51**, 5101-5105.
42.C. Pan, R. Yu, S. Niu, G. Zhu and Z. L. Wang, *ACS Nano*, 2013, **7**, 1803-1810.
43.S.-A. Wohlgemuth, R. J. White, M.-G. Willinger, M.-M. Titirici and M. Antonietti, *Green Chem.*, 2012, **14**, 1515.
44.Z. Wang, T. Yokoyama, H.-m. Chang and Y. Matsumoto, *J. Agric. Food Chem.*, 2009, **57**, 6167-6170.
45.H. Jin, Y. Nishiyama, M. Wada and S. Kuga, *Colloids and Surfaces A: Physicochem. Engin. Aspects*, 2004, **240**, 63-67.
46.R. Gavillon and T. Budtova, *Biomacromolecules*, 2007, **9**, 269-277.
47.T. Mehling, I. Smirnova, U. Guenther and R. H. H. Neubert, *J. Non-Cryst. Solids*, 2009, **355**, 2472-2479.
48.O. Ishida, D. Y. Kim, S. Kuga, Y. Nishiyama and R. M. Brown, *Cellulose*, 2004, **11**, 475-480.
49.J. Cai, S. Kimura, M. Wada, S. Kuga and L. Zhang, *ChemSusChem*, 2008, **1**, 149-154.
50. J. Cai and L. Zhang, *Macromol. Biosci.*, 2005, **5**, 539-548.
51.B. Kong, J. Tang, Z. Wu, J. Wei, H. Wu, Y. Wang, G. Zheng and D. Zhao, *Angew. Chem. Int. Ed. Engl.*, 2014, **53**, 2888-2892.
52.J. Wang, Z. Shi, J. Fan, Y. Ge, J. Yin and G. Hu, *J. Mater. Chem.*, 2012, **22**, 22459.
53.Z. Sui, Q. Meng, X. Zhang, R. Ma and B. Cao, *J. Mater. Chem.*, 2012, **22**, 8767-8771.
54.M. Rafatullah, O. Sulaiman, R. Hashim and A. Ahmad, *J. Hazard. Mater.*, 2010, **177**, 70-80.
55.V. K. Gupta and Suhas, *J. Environ. Manag.*, 2009, **90**, 2313-2342.
56.F. He, W. Wang, J.-W. Moon, J. Howe, E. M. Pierce and L. Liang, *ACS Appl. Mater. Interfaces*, 2012, **4**, 4373-4379.
57.V. Chandra, J. Park, Y. Chun, J. W. Lee, I.-C. Hwang and K. S. Kim, *ACS Nano*, 2010, **4**, 3979-3986.
58.R. Chen, H. Tanaka, T. Kawamoto, M. Asai, C. Fukushima, M. Kurihara, M. Ishizaki, M. Watanabe, M. Arisaka and T. Nankawa, *ACS Appl. Mater. Interfaces*, 2013, **5**, 12984-12990.
59.A. M. Liu, K. Hidajat, S. Kawi and D. Y. Zhao, *Chem. Commun.*, 2000, 1145-1146.
60.W. Jiang, W. Wang, B. Pan, Q. Zhang, W. Zhang and L. Lv, *ACS ACS Appl. Mater. Interfaces*, 2014, **6**, 3421-3426.

